M. M. Elsayed

A. J. Chamkha

Mechanical and Industrial Engineering Department, Kuwait University, P.O. Box 5969, Safat 13060, Kuwait

Analysis and Performance of Radial Flow Rotary Desiccant Dehumidifiers

A model is developed to predict the steady periodic performance of a radial flow desiccant wheel. The model is expressed in terms of the same dimensionless parameters that are commonly used in modeling of the conventional axial flow desiccant wheel. In addition a dimensionless geometrical ratio of the volume of the matrix to the volume of the wheel core is found to affect the performance of the wheel. A finite difference technique on staggered grid is used to discretize the governing dimensionless equations. The discretized equations are solved to predict the performance of the desiccant wheel at given values of operation parameters. A sensitivity study is carried out to investigate the effect of changing any of these parameters on the performance of the wheel. The performance of the radial flow desiccant wheel is compared with that of the convential axial flow desiccant wheel having the same values of the operation parameters.

1 Introduction

Rotary desiccant wheels have been investigated by many researchers as an option for air dehumidification in conventional air conditioning systems or in industrial air drying systems. In these wheels two streams of air are flowing in parallel or in a counter flow configuration in directions parallel to the axis of the wheel. The first air stream is process air, i.e., the air to be dehumidified, and the second air stream is the regeneration air stream. This regeneration air stream is externally heated by a heat source (solar, gas burner, etc.) before it enters the desiccant wheel to regenerate its desiccant material. This type of flow configuration is referred to as an axial flow desiccant wheel in comparison with a radial flow desiccant wheel, where the process and regeneration air streams are flowing in the radial direction instead of the axial direction.

Axial flow desiccant wheels are thoroughly investigated in the literature. The effectiveness technique to compute the outlet conditions from the wheel were introduced by Maclaine-Cross and Banks (1972), Banks (1985a, b), and Van den Bulck et al. (1985a, b). Pseudo steady-state models and finite difference models have been developed and used to study the performance of the wheel at different parametric conditions; e.g., Holmberg (1979), Aly et al. (1988), and Schultz and Mitchell (1989). More detailed work related to the performance of axial flow desiccant wheels is also given by Banks (1972a, b), Jurinak and Mitchell (1984), Jurinak et al. (1984), Epstein et al. (1985), Van den Bulck et al. (1986), Van den Bulck et al. (1988), Kang and Maclaine-Cross (1989), Collier and Cohen (1991), Chant and Jeter (1995), and Zheng et al. (1995).

Radial flow desiccant wheels have not been investigated in the literature to the best of our knowledge. In the present work, a finite difference model is developed to predict the performance of these types of heat and mass exchangers. The model is formulated using the same parameters previously introduced in the literature for modeling of the axial flow desiccant wheels. This makes it possible to compare the performance of both wheels at given values of the design and operation parameters.

Contributed by the Solar Energy Division of THE AMERICAN SOCIETY OF MECHANICAL ENGINEERS for publication in the ASME JOURNAL OF SOLAR ENERGY ENGINEERING. Manuscript received by the ASME Solar Energy Division, July 1995; final revision, July 1996. Associate Technical Editor: W. M. Worek.

2 Mathematical Model

The present analysis is presented only for the heat and mass transfer aspects of a desiccant dehumidifier without considering the pressure losses.

2.1 Differential Equations. Consider a desiccant wheel of inner radius r_1 and outer radius r_2 (see Fig. 1). The wheel is divided into two periods: period 1 of fraction β_1 of total volume of the wheel, and period 2 of fraction β_2 of total volume of the wheel ($\beta_1 + \beta_2 = 1$). Regeneration air and dehumidified air in period 1 and 2 flow radially in the inward or outward direction, respectively. The wheel rotates at a uniform rotational speed N. Using the same assumptions given by Van den Bulck et al. (1985a, 1986) for axial flow wheel, the mass and energy balances are carried out. The moisture balance of the air flowing through the control volume (CV) yields

$$\dot{m}_i \frac{dA_i}{A_i} \frac{\partial \omega}{\partial r} dr - \rho_a h_{Di} A_s dA_i dr(\omega^* - \omega) = 0 \tag{1}$$

where the meanings of the various symbols are given in the nomenclature list. Also, the moisture balance for the air flow and the rotating matrix through the CV gives the following relation:

$$\dot{m}_i \frac{dA_i}{A_i} \frac{\partial \omega}{\partial r} dr + MN \frac{2\pi r dr}{\pi(r_2^2 - r_1^2)} \frac{\partial W}{\partial t} dt = 0. \tag{2}$$

Similarly, the energy balances for the air flowing through the CV and for the air and matrix across the CV, respectively, yield

$$\dot{m}_i \frac{dA_i}{A_i} \frac{\partial h_a}{\partial r} dr - h_i A_s dA_i dr(T_m - T) + \rho_a h_{Di} A_s dA_i dr h_v(\omega^* - \omega) = 0 \tag{3}$$

$$MN \frac{2\pi r dr}{\pi(r_2^2 - r_1^2)} \frac{\partial h_m}{\partial t} dt + \dot{m}_i \frac{dA_i}{A_i} \frac{\partial h_a}{\partial r} dr = 0. \tag{4}$$

The mass transfer coefficient h_D and the heat transfer coefficient h are dependent on the superficial air velocity u within a matrix cross-sectional area. They are related to this velocity as follows (Pla-Barby et al., 1978):

$$h_D = C_m u^a, \quad h = C_h u^a \tag{5}$$

where C_m, C_h, and a are constants. In radial flow desiccant

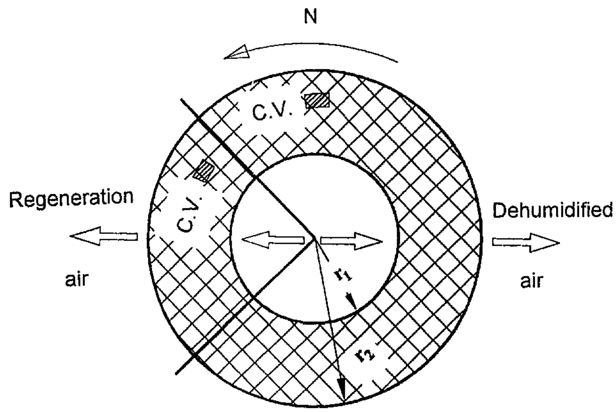

Fig. 1 Radial flow desiccant wheel

wheels, since the mass is conserved, the velocity u is inversely related to the cross-sectional flow area of the matrix at a given radius r. Therefore one may write

$$\frac{h_D}{(h_D)_r} = \left(\frac{r_r}{r}\right)^a, \quad \frac{h}{(h)_r} = \left(\frac{r_r}{r}\right)^a \tag{6}$$

where the subscript r indicates at a reference radius. For convenience the reference radius r_r is taken as r_1.

The dimensionless radius R and dimensionless time τ are defined as follows:

$$R = r/r_1, \quad \tau = Nt. \tag{7}$$

Following previous work on axial desiccant wheel (Brandemuehl and Banks, 1984; Van den Bulck et al., 1985a, b, 1986; and Schultz and Mitchell 1989), the following dimensionless parameters are introduced:

$$\Gamma_i = MN/\dot{m}_i, \quad \mathrm{NTU}_{mi} = \rho_a(h_{Di})_r A_s V \beta_i/\dot{m}_i,$$
$$\mathrm{NTU}_{hi} = (h_i)_r A_s V \beta_i/(\dot{m}_i c_{pai}) \tag{8}$$

where $(h_{Di})_r$ and $(h_i)_r$ are the mass transfer coefficient and the heat transfer coefficient for period i taken at reference radius (i.e., at $r = r_1$), respectively. A new dimensionless parameter α is now introduced for the radial flow desiccant wheel as follows:

$$\alpha = \frac{\text{volume of matrix}}{\text{volume of core}} = (R_2^2 - 1). \tag{9}$$

The governing equations given by Eqs. (1) to (4) are then reduced to the following:

$$\left.\begin{aligned}
&\frac{\partial\omega}{\partial R} - \frac{2}{\alpha}\mathrm{NTU}_{mi}R^{1-a}(\omega^* - \omega) = 0\\
&\frac{\partial W}{\partial\tau} + \frac{\alpha}{2R}\frac{1}{\Gamma_i\beta_i}\frac{\partial\omega}{\partial R} = 0\\
&\frac{\partial h_a}{\partial R} - \frac{2}{\alpha}\mathrm{NTU}_{hi}\beta_i R^{1-a}c_{pa}(T_m - T)\\
&\qquad - \frac{2}{\alpha}\mathrm{NTU}_{mi}\beta_i R^{1-a}h_v(\omega^* - \omega) = 0\\
&\frac{\partial h_m}{\partial\tau} + \frac{\alpha}{2R}\frac{1}{\Gamma_i\beta_i}\frac{\partial h_a}{\partial R} = 0
\end{aligned}\right\}. \tag{10}$$

2.2 Boundary Conditions and Property Relations. To solve Eqs. (10), boundary conditions for air flow in both periods must be specified in addition to the periodic condition for the matrix. The boundary conditions become

$$\begin{aligned}
\omega(R,\tau) &= \omega_{11} \quad R = b, \quad 0 \le \tau \le \beta_1\\
T(R,\tau) &= T_{11} \quad R = b, \quad 0 \le \tau < \beta_1\\
\omega(R,\tau) &= \omega_{21} \quad R = b, \quad \beta_1 \le \tau < 1\\
T(R,\tau) &= T_{21} \quad R = b, \quad \beta_1 \le \tau < 1
\end{aligned} \tag{11}$$

where b is a flow direction parameter such that $b = 1$ for flow in the outward radial direction and $b = R_2$ for flow in the inward radial direction. The periodic matrix conditions are given as follows:

$$W(R,0) = W(R,1), \quad T_m(R,0) = T_m(R,1) \tag{12}$$

The relations to determine the equilibrium humidity ratio ω^*

Nomenclature

A_i = cross-sectional area of flow for period i at a given location in the wheel
A_s = heat and mass transfer area per unit volume of matrix
a = constant defined by Eq. (5)
c_p = specific heat
h_a = enthalpy of moist air
h = heat transfer coefficient
h_D = mass transfer coefficient
h_{fg} = latent heat of evaporation of water
$h_{fg,0}$ = latent heat of evaporation of water at 0°C
h_m = enthalpy of matrix
h_v = enthalpy of water vapor
L = width of wheel
Le = Lewis number
$\dot{m}$ = mass flow rate
M = mass of the matrix
N = rotational speed of the desiccant wheel
N_h = number of nodes occupied by hot air
N_R = number of nodes in the R direction
N_T = total number of nodes
NTU_h = number of transfer units for heat transfer
NTU_m = number of transfer units for mass transfer
Q_H = rate of heating of regeneration air
R = dimensionless radius defined by Eq. (7)
r = radius
r_1 = inner radius of wheel
r_2 = outer radius of wheel
T = temperature
t = time
u = superficial air velocity within a matrix cross-sectional area
V = matrix volume
W = moisture content of desiccant
α = dimensionless parameter defined by Eq. (9)
β_i = fraction of total wheel volume assigned to period i
Γ = dimensionless parameter defined by Eq. (8)
η = efficiency defined by Eq. (26)
ρ = density
τ = dimensionless time defined by Eq. (7)
ω = humidity ratio of air

Superscripts

* = equilibrium condition between air and desiccant

Subscripts

a = air
av = average
m = matrix
i = inner, or inlet also, order of period ($i = 1$ for hot air period, $i = 2$ for cold air period)

Table 1 Flow configuration in the radial flow exchanger

Configuration	Direction of process air	Direction of regeneration air
1	Outward	Outward, i.e., parallel flow
2	Outward	Inward, i.e., counter flow
3	Inward	Outward, i.e., parallel flow
4	Inward	Inward, i.e., counter flow

Table 2 Basic air inlet conditions and operational parameters

Outdoor air at $T_\infty = 30°C$, $\omega_\infty = 0.014$ kgw/kga
Process air: ventilation mode $T_{21} = T_\infty$, $\omega_{21} = \omega_\infty$
recirculation mode $T_{21} = 25°C$, $\omega_{21} = 0.01$ kgw/kga
Flow configuration: 2

Operational parameters: ideal exchanger
$\Gamma_1 = \Gamma_2 = 0.2$ $\alpha = 3$
$\beta_1 = \beta_1 = 0.5$ $\Delta T = 40°C$

Operational parameters: actual exchanger
same data for ideal exchanger, and
$NTU_{h1} = NTU_{h2} = 0.1$ to 20
Le = 1.0

of air in contact with a silica gel matrix, the enthalpy of the silica gel, and the properties of moist air are given by Van den Bulck et al. (1985b) and ASHRAE (1995).

3 Finite Difference Formulation

The governing equations are solved numerically using the finite difference methodology. All derivatives with respect to either R or τ are replaced by two-point forward difference formulae. In addition, all nonderivative variables (such as R, ω, W, ω^*, T, and T_m) appearing in these equations are evaluated at the midpoint between the current and the next points in the marching direction. A staggered mesh representing the $R-\tau$ plane (similar to that used by Holmberg, 1979) has been employed. After discretization of Eqs. (10) and rearranging, the difference equations using constant step sizes in R and τ directions become

$$\omega_{k+1,l} = A_1\omega_{k,l} + A_2 R_{av}^{1-a} w_{av}^* \quad (13)$$

$$W_{k,l+1} = W_{k,l} - B(\omega_{k+1,l} - \omega_{k,l}) \quad (14)$$

$$h_{a,k+1,l} = h_{a,k,l} + C\Delta T_{av} R_{av}^{1-a} + Dh_v \Delta\omega_{av} R_{av}^{1-a} \quad (15)$$

$$h_{m,k,l+1} = h_{m,k,l} - B(h_{a,k+1,l} - h_{a,k,l}) \quad (16)$$

where

$$\left.\begin{aligned} A_1 &= \left(1 - \frac{\Delta R \mathrm{NTU}_{mi} R_{k,l}^{1-a}}{\alpha}\right) \bigg/ \left(1 + \frac{\Delta R \mathrm{NTU}_{mi} R_{k+1,l}^{1-a}}{\alpha}\right) \\ A_2 &= \left(\frac{2\Delta R \mathrm{NTU}_{mi} R_{av}^{1-a}}{\alpha}\right) \bigg/ \left(1 + \frac{\Delta R \mathrm{NTU}_{mi} R_{k+1,l}^{1-a}}{\alpha}\right) \\ R_{av}^{1-a} &= \tfrac{1}{2}(R_{k+1,l}^{1-a} + R_{k,l}^{1-a}),\ \omega_{av}^* = \tfrac{1}{2}(\omega_{k,l}^* + \omega_{k,l+1}^*) \end{aligned}\right\} \quad (17)$$

and

$$\left.\begin{aligned} B &= \frac{\Delta\tau}{2\Delta R}\frac{\alpha}{\Gamma_i \beta_i R_{av}},\quad C = \frac{2\Delta R \beta_i \mathrm{NTU}_{hi} c_{pa}}{\alpha} \\ D &= \frac{2\Delta R \beta_i \mathrm{NTU}_{mi}}{\alpha} \end{aligned}\right\}. \quad (18)$$

It is of interest to determine the temperature distribution of air and matrix in the desiccant. For this reason, Eqs. (15) and (16) are written in terms of T_a and T_m, respectively. This is accomplished by substituting the following expressions for h_a and h_m:

$$h_a = c_{pa}T + (h_{fg,0} + c_{pv}T)\omega$$

$$h_m = c_{pm}T_m + 0.221(h_{fg,0} + c_{pv}T)[\exp(-10.28\,W) - 1] \quad (19)$$

into Eqs. (15) and (16) and then rearranging to give

$$T_{k+1,l} = E_1 T_{k,l} + E_2(\omega_{k,l} - \omega_{k+1,l}) + E_3 T_{m,av} + E\Delta(R\omega)_{av} \quad (20)$$

$$T_{m,k,j+1} = T_{m,k,j+1} + \frac{1}{c_{pm}}(f_{k,l}^0 - f_{k,l+1}^0) + G(h_{a,k+1,l} - h_{a,k,l}) \quad (21)$$

where

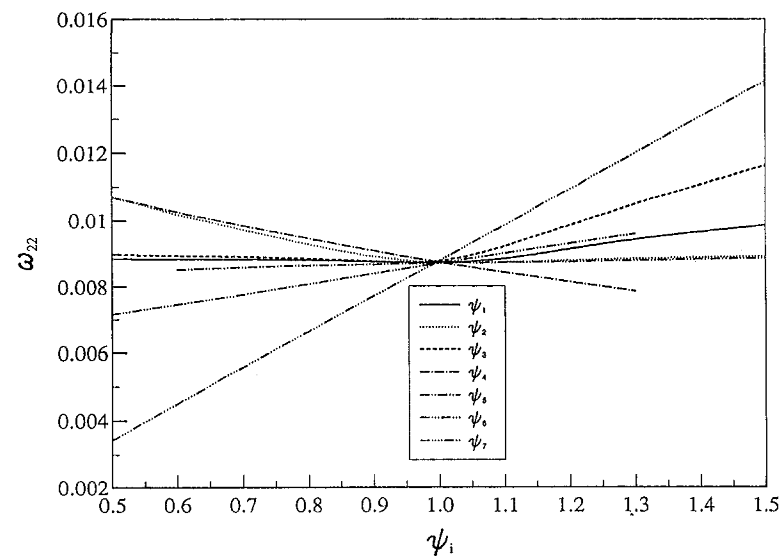

Fig. 2 Dependence of ω_{22} of an ideal radial exchanger on the inlet air condition and the operational parameters for flow configuration 2 at ventilation mode

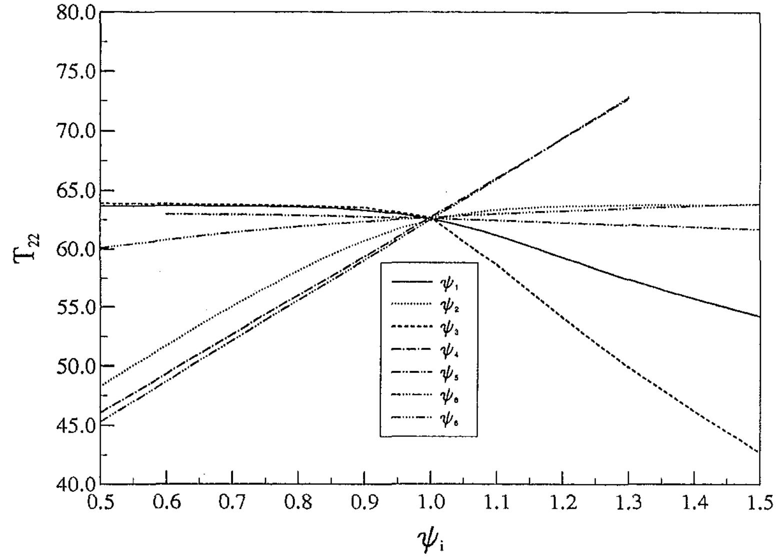

Fig. 3 Dependence of T_{22} of an ideal radial exchanger on the inlet air condition and the operational parameters for flow configuration 2 at ventilation mode

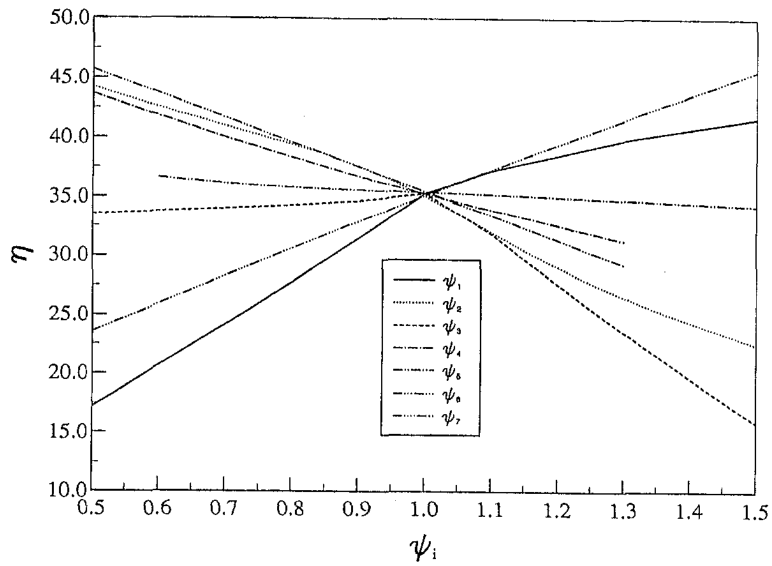

Fig. 4 Dependence of η_{22} of an ideal radial exchanger on the inlet air condition and the operational parameters for flow configuration 2 at ventilation mode

Table 3 Effect of varying Ψ_i on the values of ω_{22}, T_{22}, and η for flow configuration 2 with ventilation or recirculation modes

		Ventilation mode			Recirculation mode				Ventilation mode			Recirculation mode		
Ψ_i	Increasing	ω_{22}	T_{22}	η	ω_{22}	T_{22}	η	Decreasing	ω_{22}	T_{22}	η	ω_{22}	T_{22}	η
Ψ_1	Γ_1	+	−	+	+	−	+	Γ_1	~	~	− −	~	~	− −
Ψ_2	Γ_2	~	~	− −	~	~	− −	Γ_2	+	− −	++	++	− −	++
Ψ_3	β_1	++	− −	− −	++	− −	− −	β_1	~	~	~	~	~	−
Ψ_4	ΔT	− −	++	−	− −	++	−	ΔT	+	− −	++	++	− −	+
Ψ_5	α	~	~	~	~	~	~	α	~	~	~	~	~	~
Ψ_6	T_∞	+	++	−	+	++	+	T_∞	−	− −	++	+	− −	− −
Ψ_7	ω_∞	++	~	++	+	~	−	ω_∞	− −	~	− −	−	+	+

++ = strongly increased: + = increased: − − = strongly decreased: − = decreased: ~ = weak or negligible effect.

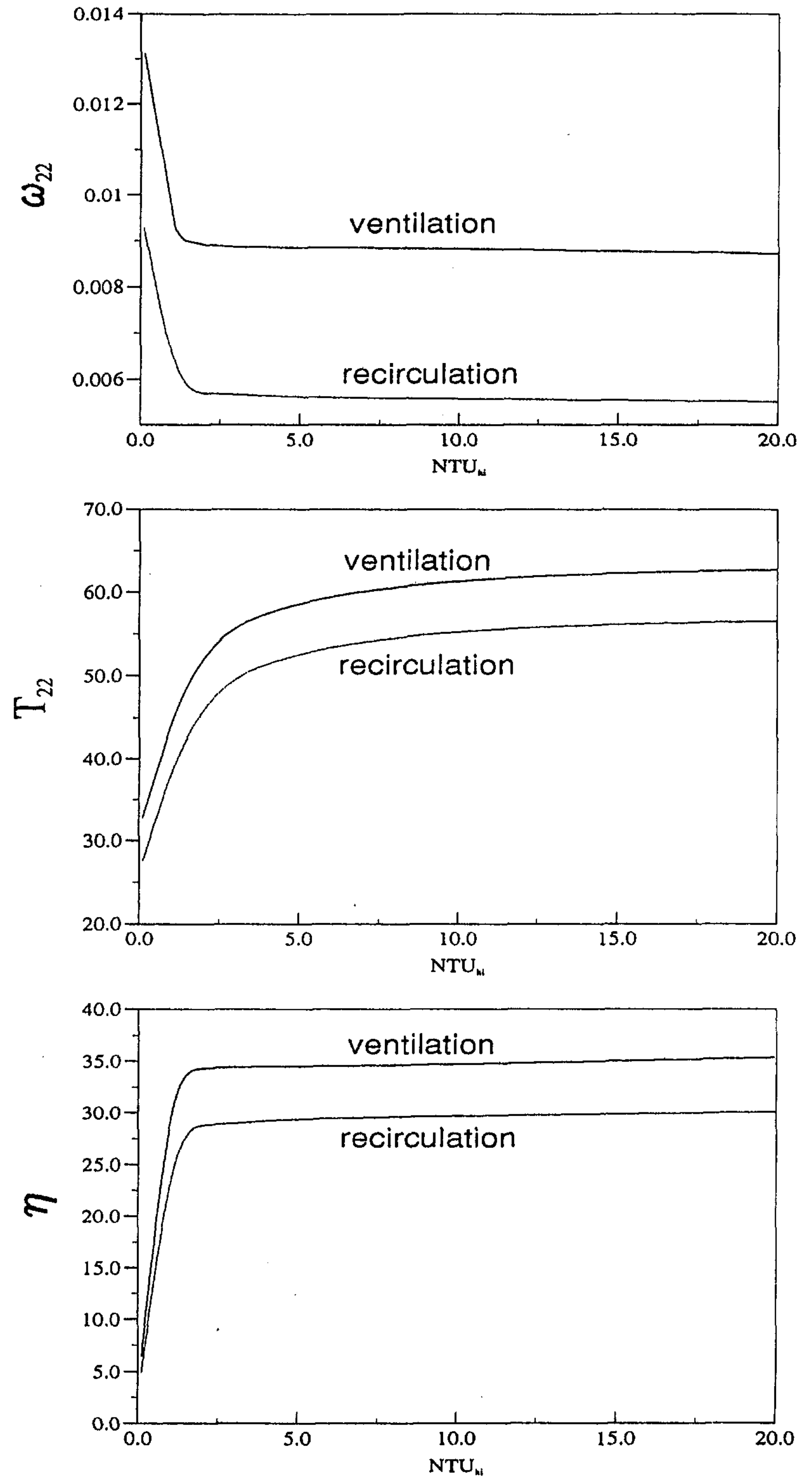

Fig. 5 Dependence of performance of radial exchanger on the value of NTU_{hl}

$$\left.\begin{aligned} E_1 &= (c_{pa} + c_{pv}\omega_{k,l} - \tfrac{1}{2}CR_{k,l}^{1-a})/E_0 \\ E_0 &= c_{pa} + c_{pv}\omega_{k+1,l} + \tfrac{1}{2}CR_{k+1,l}^{1-a} \\ E_2 &= h_{fg,0}/E_0, \quad E_3 = \tfrac{1}{2}CR_{av}^{1-a}/E_0 \\ E_4 &= Dh_v R_{av}^{1-a}/E_0 \end{aligned}\right\} \tag{22}$$

and

$$\begin{aligned} f^0 &= 0.221\ h_{fg,0}(\exp(-10.28W) - 1) \\ G &= B/c_{pm}. \end{aligned} \tag{23}$$

The above equations are applicable for both the hot air side and the cold air side. The boundary conditions for air and the periodic matrix conditions in difference form are as follows:

$$\left.\begin{aligned} &\omega(b, l) = \omega_{11}, \quad T(b, l) = T_{11}, \quad l = 1, 2, \ldots N_h \\ &\omega(b, l) = \omega_{21}, \quad T(b, l) = T_{21}, \quad l = N_h + 1, \ldots N_T \\ &W(k, l) = W(k, N_T), \quad T_m(k, 1) = T_m(k, N_T), \\ &\qquad\qquad\qquad\qquad k = 1, 2, \ldots N_R \end{aligned}\right\}. \tag{24}$$

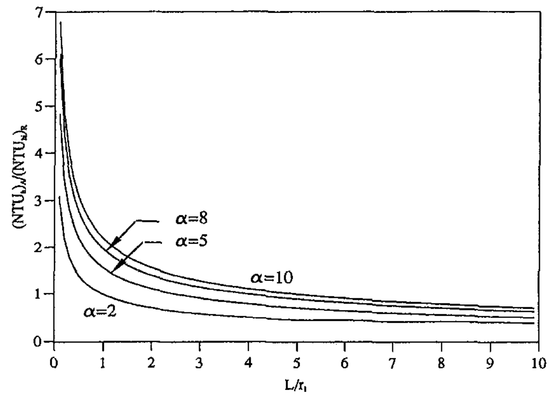

Fig. 6 Variation of the ratio of $(NTU_h)_A/(NTU_{hi})_R$ with α and L/r_1

The difference equations along with the difference conditions presented earlier are solved with iteration being employed to deal with the nonlinearities of these equations. At each iteration, an under-relaxation procedure is employed and both mass and energy balances are met. A convergence criterion based on the percentage difference between the current and the previous iterations was employed. This percentage of error was set to 1 percent in the present work. The effect of the values of ΔR and $\Delta \tau$ are tested. Solutions are obtained with continuous refinement of ΔR and $\Delta \tau$ until the solution became independent of the this refinement.

Of special importance are the outlet humidity ratio and temperature of air on the cold side (period 2) of the dehumidifier. The mean values for these variables are calculated using

$$\omega_{22} = \frac{1}{N_T - N_h} \sum_{j=N_h}^{N_{T-1}} (\omega_{22,j})_{\text{outlet}},$$

$$\bar{T}_{22} = \frac{1}{N_T - N_h} \sum_{j=N_h}^{N_{T-1}} (T_{22,j})_{\text{outlet}}. \quad (25)$$

4 Performance of Radial Flow Exchanger

Consider a radial flow exchanger with process air at (T_{21}, ω_{21}) is dehumidified to state (T_{22}, ω_{22}). Regeneration air at ambient state (T_∞, ω_∞) is preheated to state (T_{11}, ω_{11}) before it is introduced to the exchanger. The rate of heating of the regeneration air is

$$Q_H = \dot{m}_1 c_{pa1}(T_{11} - T_\infty) = \dot{m}_1 c_{pa1}\Delta T \quad (26)$$

where ΔT is the temperature rise in the heater. The efficiency of the dehumidification process by solid desiccant is now defined as follows:

$$\eta = \frac{\dot{m}_2 h_{fg}(\omega_{21} - \omega_{22})}{Q_H}. \quad (27)$$

Using Eq. (26), the above equation becomes

$$\eta = \frac{\dot{m}_2}{\dot{m}_1} \frac{h_{fg}}{c_{pa1}\Delta T} (\omega_{21} - \omega_{22}). \quad (28)$$

There are four flow configurations to be applied to the radial flow exchanger. These are identified as depicted in Table 1. Also, there are three modes of operation which depend on the state of process air entering the exchanger: ventilation mode (i.e., the process air state is the same as the ambient air), recirculation mode (i.e., the process air state is the same as the design condition of the indoor air), and mixed mode (i.e., mixture of specified ratio of indoor and outdoor air).

4.1 Ideal Exchanger. In an ideal exchanger, the values of NTU_{hi} and NTU_{mi} become reasonably large, i.e., they tend to approach infinity. Under this condition, $\omega = \omega^*$, and $T_m = T$, and the governing equations reduce to

$$\frac{\partial W}{\partial \tau} + \frac{\alpha}{2R} \frac{1}{\Gamma_i \beta_i} \frac{\partial \omega}{\partial R} = 0 \quad (29)$$

$$\frac{\partial h_m}{\partial \tau} + \frac{\alpha}{2R} \frac{1}{\Gamma_i \beta_i} \frac{\partial h_a}{\partial R} = 0. \quad (30)$$

To predict the performance of the exchanger, consider the basic values of air inlet conditions and operational parameters given in Table 2. A sensitivity study is carried out to predict the performance dependence on the change of any one of these values while the others are kept constant at their basic values. For convenience, the variable ψ_i is defined as

$$\psi_i = \frac{Z_i}{(Z_i)_b} \quad (31)$$

where b refers to basic value, Z stands for the parameter to be changed, and $i = 1$ refers to Γ_1, $i = 2$ refers to Γ_2, $i = 3$ refers to β_1, $i = 4$ refers to ΔT, $i = 5$ refers to α, $i = 6$ refers to T_∞, $i = 7$ refers to ω_∞.

Figures 2 to 4 demonstrate the variation of ω_{22}, T_{22} and η with the change of ψ_i for flow configuration 2, for ventilation mode. Results of recirculation modes are also obtained but not shown herein due to space limitation. Table 3 summarizes the effects of these changes. From the table one may conclude the following:

(a) In either ventilation mode or recirculation mode, the lowest value of ω_{22} is obtained by increasing ΔT and/or when ω_∞ is decreased. The efficiency is improved by increasing ΔT.

(b) As ω_∞ increases the dehumidification efficiency is increased for ventilation mode, and it is decreased for recirculation mode.

(c) As T_∞ increases the dehumidification efficiency is decreased for ventilation mode and is increased recirculation mode.

4.2 Actual Exchanger. Unlike the ideal exchanger, the actual exchanger has finite values of NTU_{hi} and NTU_{mi}. The air inlet conditions and the operational parameters are assigned the values given in Table 2, but NTU_h is changed from 0.1 to 20 with the assumption that $Le = 1.0$. The effect of changing the value of NTU_h on ω_{22}, T_{22} and η is depicted in Fig. 5. The following is concluded from the figure:

(a) As NTU_h is increased beyond 2, ω_{22} and η are not affected. This means that at $NTU_h \geq 2.0$ the exchanger may be treated as an ideal exchanger. However, this is not true for T_{22} which is increased as NTU_h is increases. The increase in T_{22} becomes negligible when NTU_h is increased beyond 10.

(b) For the inlet air conditions in Table 2, the dehumidification efficiency for the ventilation mode is always higher than that for the recirculation mode.

5 Comparison of Radial Flow Exchanger With Axial Flow Exchanger

A question may now arise: which exchanger has better performance, an axial flow exchanger or a radial flow exchange? To answer this question, the dimensions of the exchanger must be the same. Also, the values of Γ_1, Γ_2, and β_1 must be taken the same for both exchanger. Here it is assumed that both the axial flow and radial flow dehumidifiers have the same rotational speed, the same fraction of total wheel volume is assigned to the hot air period (i.e., same values of β_1 and β_2) and the same values of the ratios of Γ_1 and Γ_2. The values of NTU_{hi} and

NTU_{mi} are not, however, the same. The values of NTU_{hi} and NTU_{mi} for axial flow exchangers are defined as follows:

$$(NTU_{hi})_A = (h_i)_A A_s V \beta_i / (\dot{m}_i \cdot c_{pai}),$$
$$(NTU_{mi})_A = \rho_a (h_{Di})_A A_s V \beta_i / \dot{m}_i \qquad (32)$$

where $(h_i)_A$ and $(h_{Di})_A$ refer to heat transfer and mass transfer coefficients, respectively, for axial flow exchanger. Using Eqs. (8) and (32) give

$$\frac{(NTU_{hi})_R}{(NTU_{hi})_A} = \frac{(h_i)_A}{(h_{i,r_1})_R} \qquad (33)$$

where the subscripts A and R refer to axial and radial exchangers, respectively, and the subscript r_1 refer to at radius r_1 in case of radial flow exchanger.

Substituting Eq. (5) into (33) and replacing the superficial velocity by its expression in terms of the mass flow rate and cross section flow area yield

$$\frac{(NTU_{hi})_A}{(NTU_{hi})_R} = [\tfrac{1}{2}\alpha/(L/r_1)]^a \qquad (34)$$

where $a = 0.49$ as reported by Pla-Barby et al. (1978). For $Le = 1$, we also write

$$\frac{(NTU_{mi})_A}{(NTU_{mi})_R} = [\tfrac{1}{2}\alpha/(L/r_1)]^a. \qquad (35)$$

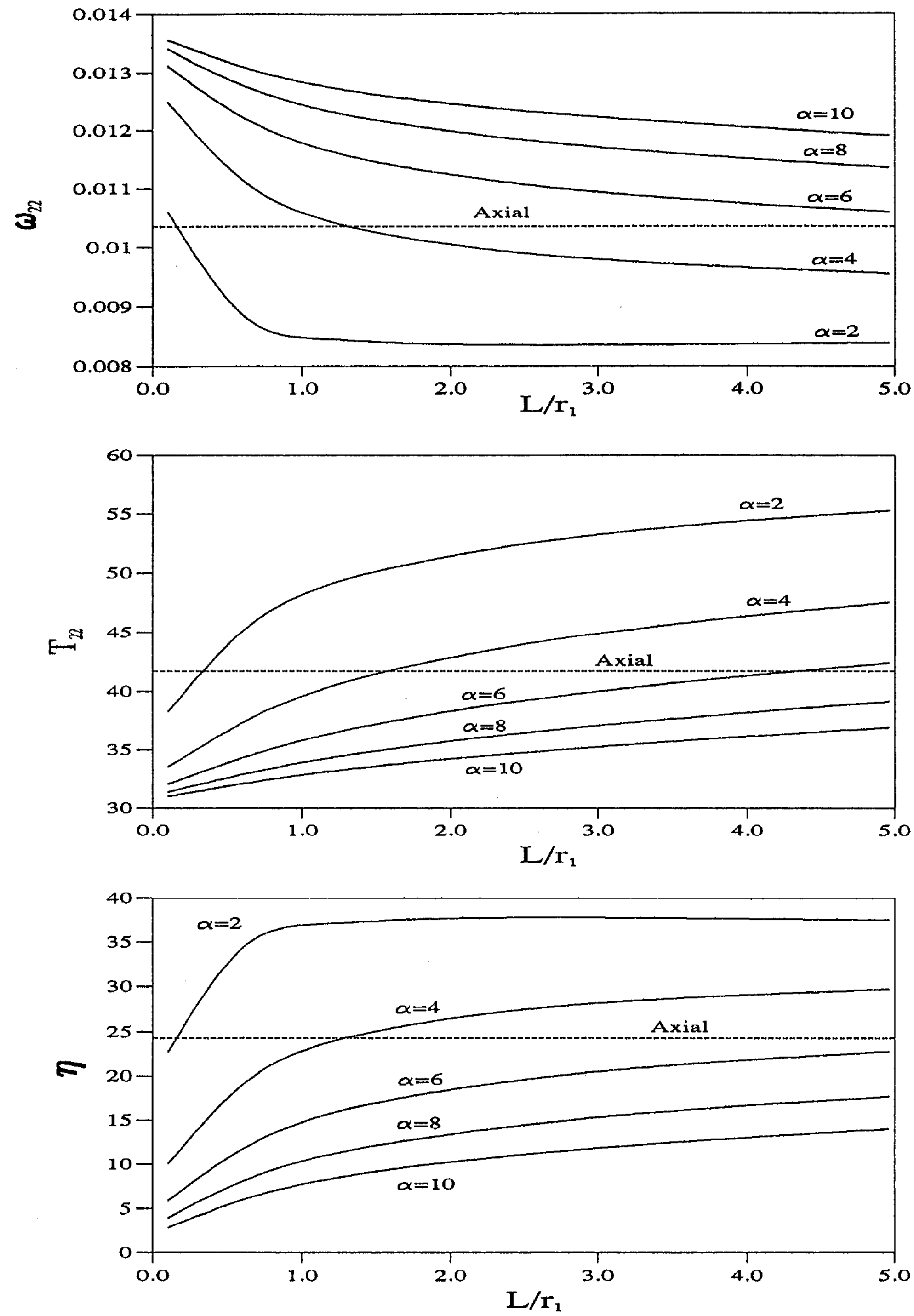

Fig. 7 Comparison of performance of radial exchanger at ventilation mode for $(NTU_h)_A = 1.0$ and various values of α and L/r_1

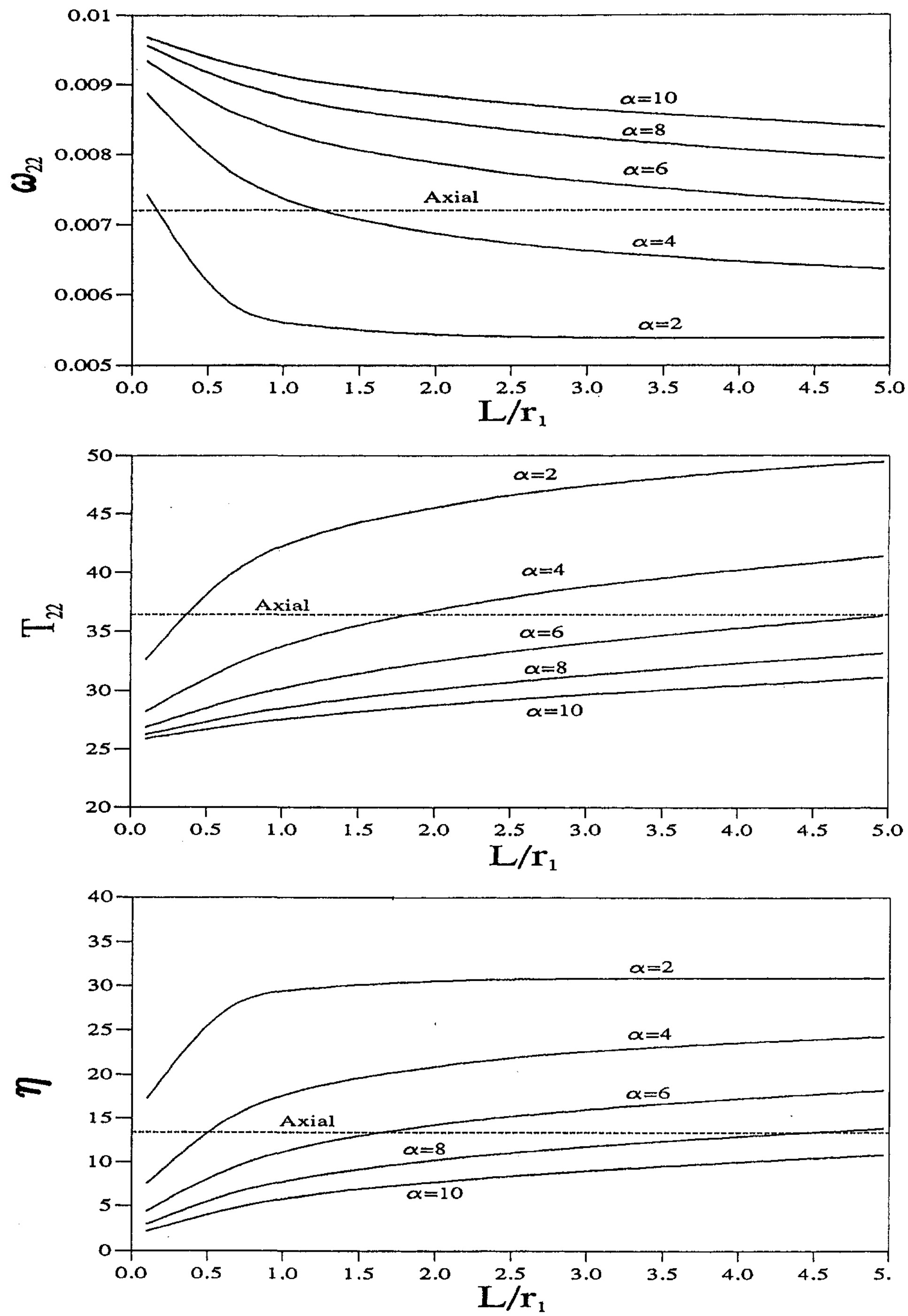

Fig. 8 Comparison of performance of radial exchanger with axial exchanger at recirculation mode for $(\mathrm{NTU}_h)_A = 1.0$ and various values of α and L/r_1

Figure 6 shows a plot of Eqs. (34) and (35) at various values of α and L/r_1. As shown in the figure the ratio of $(\mathrm{NTU}_{hi})_A/(\mathrm{NTU}_{hi})_R$ is always greater than 1, when $L/r_1 \leq 1$ regardless of the value of α.

Figures 7 and 8 compare the performance of radial exchangers with axial exchangers at $(\mathrm{NTU}_h)_A = 1.0$ when operated at ventilation and recirculation modes, respectively. It is clear from these figures that the performance of the radial exchangers is fully dependent on the parameters α and L/r_1. For example in both the ventilation and recirculation modes, a radial exchanger with $\alpha = 2$ gives lower values of ω_{22} and higher values of η than axial exchanger. At $\alpha \geq 6$, the trend is the opposite, i.e., axial exchangers gives lower values of ω_{22} and higher values of η than radial exchangers.

Figure 9 shows a comparison of the variation of ω_{22} with L/r_1 for radial exchangers with that of axial exchangers, at $(\mathrm{NTU}_h)_A = 1$ and 20. Both ventilation and recirculation modes are considered with $\alpha = 4$ and 10. As shown in the figure, regardless of the value $(\mathrm{NTU}_h)_A$, ω_{22} given by a radial exchanger may be less, equal, or greater than that of an axial exchanger depending on the value of α and L/r_1.

It is now of interest to know: is a radial exchanger superior to an axial exchanger or is it the other way around? To answer this question, we need to define the criteria of superiority. One

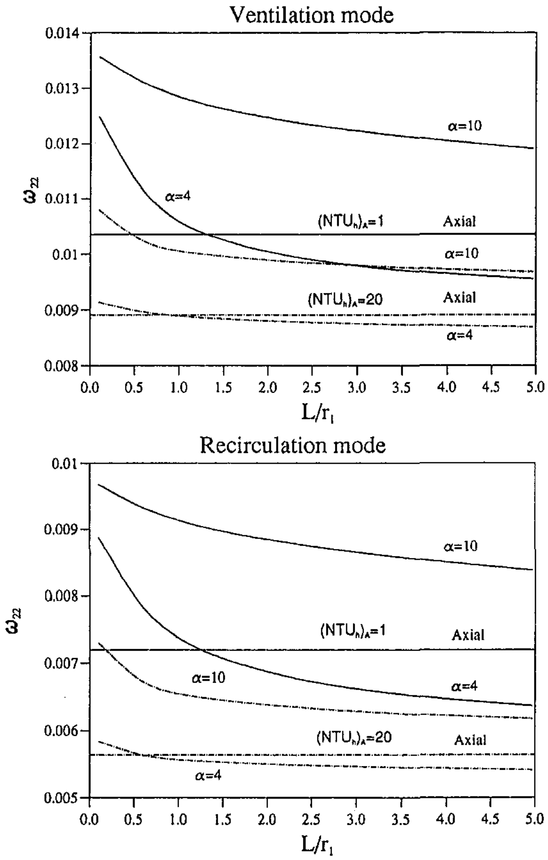

Fig. 9 Comparison of performance of radial and axial exchangers for $(NTU_h)_A = 1.0$ and 20.0 for various values of L/r_1 and α for both ventilation and recirculation modes

criterion is having low value of ω_{22} and high value of η_{22}. Another criterion is having low pressure drop of the air flowing through the exchanger. In the first criterion, Figs. 7 to 9 show that as α decreases and L/r_1 increases beyond certain limits, radial exchangers become superior to axial ones. Fortunately, this also satisfies the second criterion of lower pressure drop where the pressure drop decreases as α decreases. More detailed work should be carried out in this direction.

6 Conclusion

Radial flow desiccant wheel is modeled using the same dimensionless parameters used in modeling of conventional axial flow desiccant wheel. The comparison of the performance of both wheels showed that either one of these wheels may become superior to the other depending on the values of the design and operating parameters.

References

Aly, S. E., Fathalah, K., and Gari, H. A., 1988, "Analysis of an integrated vapor compression and waste heat dehumidifier A/C system," *Heat Recovery Systems & CHP*, Vol. 8, No. 6, pp. 503–528.

Banks, P. J., 1972B, "Coupled equilibrium heat and single adsorbate transfer in fluid flow through a porous medium—II. Predictions for silica-gel air-drier using characteristic charts," *Chemical Engineering Science*, Vol. 27, pp. 1157–1169.

Banks, P. J., 1972a, "Coupled equilibrium heat and single adsorbate transfer in fluid flow through a porous medium—I. Characteristic potential and specific capacity ratios," *Chemical Engineering Science*, Vol. 27, pp. 1143–1155.

Banks, P. J., 1985a, "Prediction of Heat and Mass Regenerator Performance Using Nonlinear Analogy Method: Part 1—Basis," ASME *Journal of Heat Transfer*, Vol. 107, pp. 222–229.

Banks, P. J. 1985B, "Prediction of Heat and Mass Regenerator Performance Using Nonlinear Analogy Method: Part 2—Comparison of Methods," ASME *Journal of Heat Transfer*, Vol. 107, pp. 220–238.

Brandemuehl, M. J., and Banks, P. J., 1984, "Rotary Heat Exchangers With Time Varying or Nonuniform Inlet Temperatures," ASME *Journal of Heat Transfer*, Vol. 106, pp. 750–758.

Chant, E. E., and Jeter, S. M., 1995, "On the Use of the Parabolic Concentration Profile Assumption for a Rotary Desiccant Dehumidifier," ASME JOURNAL OF SOLAR ENERGY ENGINEERING, Vol. 117, pp. 45–50.

Collier, R. K., and Cohen, B. M., 1991, "An analytical examination of methods for improving the performance of desiccant cooling systems," ASME JOURNAL OF SOLAR ENERGY ENGINEERING, Vol. 113, pp. 157–163.

Epstein, M., M., K., Grolmes, Davidson, J., and Kosar, D., 1985, "Desiccant Cooling System Performance: A Simple Approach," ASME JOURNAL OF SOLAR ENERGY ENGINEERING, Vol. 107, pp. 21–28.

Holmberg, R. B., 1979, "Combined Heat and Mass Transfer in Regenerators With Hygroscopic Materials," ASME *Journal of Heat Transfer*, Vol. 101, pp. 205–210.

Jurinak, J. J., and Mitchell, J. W., 1984, "Effect of Matrix Properties on the Performance of a Counterflow Rotary Dehumidifier," ASME *Journal of Heat Transfer*, Vol. 106, pp. 638–645.

Jurinak, J. J., Mitchell, J. W., and Beckman, W. A., 1984, "Open-Cycle Air Conditioning as an Alternative to Vapor Compression Cooling in Residential Applications," ASME JOURNAL OF SOLAR ENERGY ENGINEERING, Vol. 106, pp. 252–260.

Kang, T. S., and Macline-cross, I. L., 1989, "High performance, solid desiccant, open cooling cycles," ASME JOURNAL OF SOLAR ENERGY ENGINEERING, Vol. 111, pp. 176–183.

Maclain-cross, I. J., and Banks, P. J., 1972, "Coupled heat and mass transfer on regenerators—Prediction using an analogy with heat transfer," *Int. J. H. M. Transfer*, Vol. 15, pp. 1225–1242.

Pla-Barby, P. E., Vliet, G. C., and Pauton, R. L., 1978, "Performance of Rotary Bed Silica Gel Solid Desiccant Dryers," ASME Paper No. 78-HT-36.

Schultz, K. J., and Mitchell, J. W., 1989, "Comparison of DESSIM Model With a Finite Difference Solution for Rotary Desiccant Dehumidifiers," ASME JOURNAL OF SOLAR ENERGY ENGINEERING, Vol. 111, pp. 286–291.

Van den Bulck, E., Mitchell, J. W., and Klein, S. A., 1985a, "Design theory for rotary heat and mass exchangers—I: Wave analysis of rotary heat and mass exchangers with infinite transfer coefficients," *Int. J. Heat Mass Transfer*, Vol. 28, pp. 1575–1586.

Van den Bulck, E., Mitchell, J. W., and Klein, S. A., 1985B, "Design theory for rotary heat and mass exchangers—II: Effectiveness-number-of-transfer-units method for rotary heat and mass exchangers," *Int. J. Heat Mass Transfer*, Vol. 28, pp. 1587–1595.

Van den Bulck, E., Mitchell, J. W., and Klein, S. A., 1986, "The use of dehumidifiers in desiccant cooling and dehumidification systems," ASME *Journal of Heat Transfer*, Vol. 108, pp. 684–692.

Van den Bulck, E., Klein, S. A., and Mitchell, J. W., 1988, "Second Law Analysis of Solid Desiccant Rotary Dehumidifiers," ASME JOURNAL OF SOLAR ENERGY ENGINEERING, Vol. 110, pp. 2–9.

Zheng, W., Worek, W. M., and Novosel, D., 1995, "Performance Optimization of Rotary Dehumidifiers," ASME JOURNAL OF SOLAR ENERGY ENGINEERING, Vol. 117, pp. 40–44.